Numerical Analysis of Propulsion for Submarine with Highly Skewed Propeller

Yung-An Chu[1], Chun-Ta Lin[1], Ching-Yeh Hsin[2], Ya-Jung Lee[3]

[1]   R/D Section, Research Department, CR Classification Society, Taipei, Taiwan 10491
[2]   Dept. of Systems Engineering and Naval Architecture, National Taiwan Ocean University, Taiwan 20224
[3]   Dept. of Engineering Science and Ocean Engineering, National Taiwan University, Taiwan 10617

Abstract

Propulsion simulation of an axisymmetric submerged body in RANS coupled with propeller body force method is presented. The calm water resistance of DARPA SUBOFF model with full appendages was calculated by CFD software. A generic submarine propeller based on INSEAN E1619 was constructed to the published projected outlines and specific pitch at 70% radial position to match the experimental open water K-J chart, especially the thrust coefficient among the whole operational range. A 3D panel method of potential flow solver was utilized to calculate propeller performance, as well as providing the equivalent body forces for propulsion simulation. Comprehensive wake survey were carried out and compared with virtual disk model. The effect of various propeller loading conditions on the propulsive characteristics of the submarine model was investigated. The results of the body force approach with panel method show better agreement with other fully RANS simulation.

Keywords: Propulsion, Submarine, Body force, RANS

1. Introduction

In regards of underwater noise, submarines are commonly equipped with a highly skewed propeller. For such kind of geometry, the model and a suitable body-fitted grid in RANS will take a long time to build, so that decelerating the design process.

Huang and Groves compared the effect of interaction between the axisymmetric body and propeller through experimental approaches and calculating the asymmetric Euler equations, which gave precise predictions of the thrust deduction and the pressure distribution induced by the operating propeller. For analysis of the interaction between the wake and propeller, direct calculating the ship along with its propeller using viscous flow RANS model is the most intuitive way. However, due to the highly complicated geometry of the propeller, the need to use enormous grid numbers to resolve the flow near the propeller made the way impractical to conduct, let alone the necessity of using unsteady flow calculation. Therefore, potential flow is the most effective and efficient to calculate the propeller force, and makes both flow fields coupled with each other well. Wei(2012) numerically simulated the self propulsion of the surface ship by CFD method coupled with Body Force Method. Estimations of the self propulsion point showed a good agreement with the that of experiment method. Chase(2012) carried out a series of investigation for the DARPA SUBOFF model, including the simulations of the self-propulsion condition with INSEAN E1619 by using the overset flow solver CFDShip-Iowa V4.5. Sinan(2017) also used the same submarine and propeller model with ANSYS Fluent. Computations are validated by the published experimental data of the propeller for forward speed and forward propeller rotation and the rest of the quadrants are predicted numerically.

In the study, a variety of tests have been simulated by CFD method and 3D panel method of potential flow solver. Validation and comparison using different methods are presented.

2. Geometry Models

Details of the submarine model and propeller model used in the study are as follows:

2.1 Submarine model

Among the submarine model for the academic purpose, the DARPA SUBOFF model is the most commonly used due to a great deal of available ex-

periment data and extensive researches for validation and comparison (Liu and Huang, 1998). In the study, the AFF-8 configuration including the fairwater, and stern rudders is chose for simulation. It comprises of a fairwater which is located at the top dead center of the hull starting at x = 0.92 m from the bow and ending at x = 1.29 m as well as a cross shaped rudder where rudders and hydroplanes are located at x=4 m from the bow. The main dimensions of the computational domain are determined in accordance with the ITTC guidelines. Top view and side view of the computational domain and are given in Figure 1. Mesh of the whole computational domain was displayed in Figure 2.

Table 1 Principal particulars of DARPA **SUBOFF**

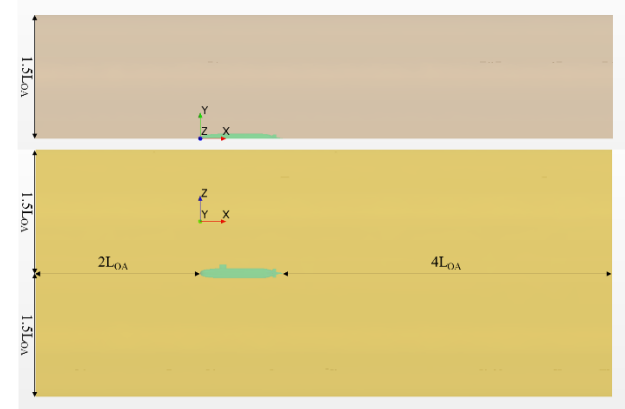| Description	Symbol	Magnitude
Length overall	L_{OA}	4.356 m
Length between perpenticulars	L_{pp}	4.261 m
Maximum hull radius	R_{max}	0.254 m
Centre of buoyancy (aft of nose)	FB	0.4621 L_{OA}
Volume of displacement		0.718 m^3
Wetted Surface	S_w	6.338 m^2
Propeller Diameter	P_D	0.262 m

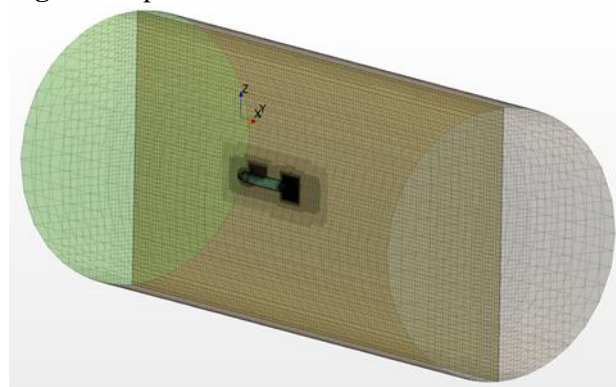**Fig. 1** Computational domain of DARPA SUBOFF

Fig. 2 Cut-away view of DARPA SUBOFF

2.2 Propeller Model

The propeller used for the study in INSEAN E1619 generic submarine propeller. The propeller is seven-blade highly skewed submarine propeller with an unloaded tip blade design and the main particulars of the submarine propeller are given in Table 1 (Di Felice et al. 2009). The propeller has been analyzed in self-propelling DARPA SUBOFF AFF-8 condition and four quadrant conditions. Open water experiments were performed in the INSEAN towing tank, and wake velocity measurements were carried out by Laser Doppler Velocimetry (LDV) system in the large circulating water channel at INSEAN. Results were presented by Di Felice et al. (2009). The main particulars of the E1619 submarine propeller are given in Table 2 and 3-D views are shown in Figure 3. However detail information about the geometry is not provided, so a parametrized tool of propeller modelling was implemented in Rhinoceros and Grasshopper. Distributions of pitch, chord length, camber, and thickness were finely tuned. In Figure 4 the propeller geometry tuned to match that of INSEAN E1619 used for the study is presented.

Table 2 Principal particulars of INSEAN E1619 submarine propeller

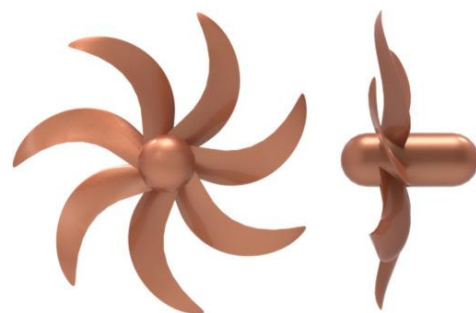| Propeller Type	INSEAN E1619
Advanced Speed	1.68 m/s
RPM	280 RPM
Diameter	0.485 m
Number of Blades	7
A_E/A_0	0.608
Hub/Diameter Ratio	0.226
Pitch/Diameter Ratio, P/D at 0.7R	1.15

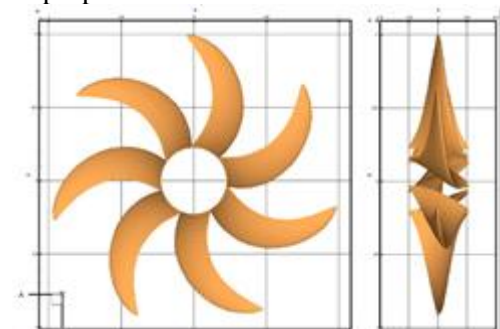**Fig. 3** 3-D views of INSEAN E1619 propeller

Fig. 4 3-D views of tuned propeller

3. Mathematical Model and Methods

3.1 RANS Method

The governing equations are the continuity equation and the well-known RANS equations for the unsteady, three dimensional and incompressible flow. The continuity can be given as:

$$\frac{\partial U}{\partial t} + \frac{\partial U_i}{\partial x_i} = 0 \tag{1}$$

While the momentum equations are expressed as:

$$\frac{\partial U}{\partial t} + \frac{\partial U_i U_j}{\partial x_j} = - \tag{2}$$

$$\frac{1}{\rho}\frac{\partial P}{\partial x_i} + \frac{\partial}{\partial x_j}\left[\upsilon\left(\frac{\partial U_i}{\partial x_j} + \frac{\partial U_j}{\partial x_i}\right)\right] - \frac{\overline{u_i' u_j'}}{\partial x_j}$$

In momentum equations, U_i and u_i' represent the mean velocity and the fluctuation velocity components in the direction of the Cartesian coordinate x_i, respectively. P, ρ and υ express the mean pressure, the density and the kinematic viscosity coefficient, respectively.

The K-ε turbulence model is employed in order to simulate the turbulence flow around the submarine model and propeller model precisely. This turbulence model is applicable when there are not high pressure changes along the form and separation near the submarine model. The K-ε turbulence model is used because the model is submerged so as to be no free surface effects. During the analysis, Reynolds stress tensor is also calculated as follow:

$$\overline{u_i' u_j'} = -\upsilon_t\left(\frac{\partial U_i}{\partial x_j} + \frac{\partial U_j}{\partial x_i}\right) + \frac{2}{3}\delta_{ij}k \tag{3}$$

where the υ_t is the eddy viscosity and can be expressed as $\upsilon_t = C_\mu k^2/\varepsilon$ whilst C_μ is an empirical constant (C_μ=0.09). The K is the turbulent kinetic energy and ε is the turbulent dissipation rate. In addition to the continuity and momentum equations, two transport equations are solved for k and ε:

$$\frac{\partial(\rho k)}{\partial t} + \frac{\partial(\rho k u_j)}{\partial x} = \frac{\partial}{\partial x_j}\left[(\mu+\frac{\mu_t}{\sigma_k})\frac{\partial k}{\partial x_j}\right] + G_k \tag{4}$$

$$+G_b - \rho\varepsilon - Y_M + S_k$$

$$\frac{\partial(\rho\varepsilon)}{\partial t} + \frac{\partial(\rho\varepsilon u_j)}{\partial x} = \frac{\partial}{\partial x_j}\left[(\mu+\frac{\mu_t}{\sigma_\varepsilon})\frac{\partial\varepsilon}{\partial x_j}\right] + \tag{5}$$

$$C_{1\varepsilon}\frac{\varepsilon}{k}(G_k + C_{3\varepsilon}G_b) - C_{2\varepsilon}\rho\frac{\varepsilon^2}{k} + S_\varepsilon$$

where $\sigma_k, G_k, G_b, Y_M, S_k, C_{1\varepsilon}, C_{2\varepsilon}, C_{3\varepsilon}$, and S_ε is the related constants and terms required in the turbulence model. Further explanations for the K-ε turbulence model can be found in the reference (D. C. Wilcox, 1993).

3.2 Determination of open water K-J chart

To evaluate the performance of propeller, it is common to conduct the propeller open water test. In the study, to reduce the time and cost of calculations, the actuator dick whose parameters has been tuned to make the open water K-J chart as matched as possible was taken into analysis, not the real geometry of the INSEAN E1619. We utilized a 3D panel method of potential flow solver, PATPAN-S to calculate the propeller force, convert the equivalent body forces for propulsion, and put it into the actuator disk element by element.

3.3 Determination of Self Propulsion Condition

Propulsion simulation was then conducted and by changing the advance coefficient to obtain the self-propulsion condition. In the study, three approaches used to derive the self-propulsion point are as follow:
A. RANS with Virtual Disk using experimental open water K-J chart. In this method, the built-in Virtual Disk module with input of the experimental open water K-J chart data was activated. The procedure for find the self propulsion point is the balance of T and Q, and then the axial and the tangential body force components are calculated so that the effects of a propeller such as thrust and torque can be modeled through the uniform volume force distribution over the cylindrical virtual disk. Further instructions for Body Force Propeller Method can be seen in the reference (SIEMENS, 2016).
 B. RANS coupled with PATPAN-S: in the calculation of the body force method, the propeller force calculated by PATPAN-S is also placed into the grid of the actuator disk in the form of force per unit volume. This does cause a change in the flow field, which makes the flow into the actuator disk varied again. Therefore, in this method, the iterative operation of the interaction between the viscous flow RANS method and the potential flow method (BEM) must be performed, and the iterative procedure is as follows:
1. Calculate the flow field around the hull using the viscous flow RANS method, and capture the velocity of the flow field in the plane of the propeller as the inflow of the propeller;
2. Solve the propeller force by using the analytical program PATPAN-S (BEM);
3. The force of the propeller is converted into the form of force per unit volume and placed in the mesh of the actuator disk; calculate the updated flow field in which the force per unit volume has been added in until the convergence of the flow field;
4. Update the inflow of the propeller, and subtract the propeller-inducing speed from the flow field velocity of the propeller plane that was captured, as an effective inflow of the propeller;
5. Repeat step 2. to 4. until the propeller force converges.

C. RANS with Virtual Disk using open water K-J chart of the tuned propeller: open water K-J chart of the tuned propeller has been input in the CFD software with Virtual Disk module activated.

4. Results

Three traditional tests in the naval architecture have been simulated and elaborated as follows:

4.1 Resistance Test

Assumption was made that the submarine model advanced in the infinite calm water so that free surface effect on the total resistance of the model was neglected. Structured mesh was generated in the whole computational domain and refinement was made where the curvature of the hull varied dramatically as well as the geometric continuity failed to be retained. Also, grid sensitivity for both the minimum and maximum tested speed as shown in Figure 6 and Figure 7 was conduct to ensure the sufficient grid numbers were produced before a series of resistance simulations were executed. The final grid number was about 13.5 million. The appropriate boundary condition could facilitate the convergence of the flow. In this part, because of the bilateral symmetry of the submarine model, half of the form was created to simplify the problem and reduce the time of analysis. Hence, the boundary conditions in the part are shown in Figure 4.

In comparison with the experimental data of DTMB (David Taylor Model Basin), the velocity interval from 3.045 m/s to 9.254 m/s was taken into consideration. Last but not the least, with the change of velocity, it was necessary to check y+ to ensure the value in accordance to reference (between 30 to 300 or so) to resolve turbulent shear layers. For v=3.045 m/s, y+ has been shown in Figure 5
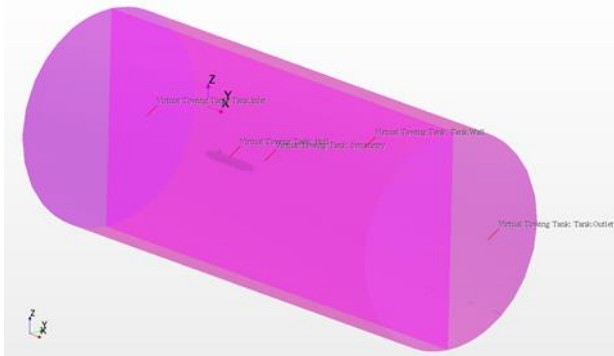

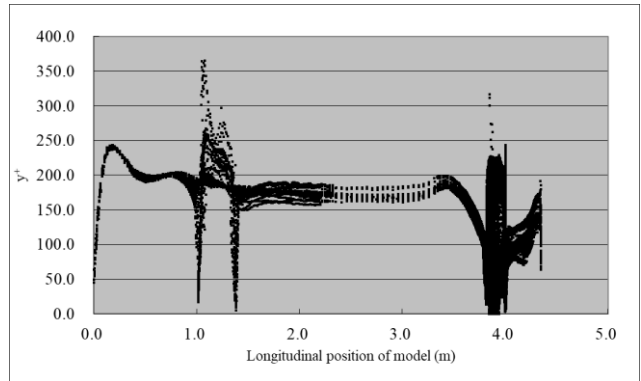**Fig. 4** Boundary conditions for resistance simulations
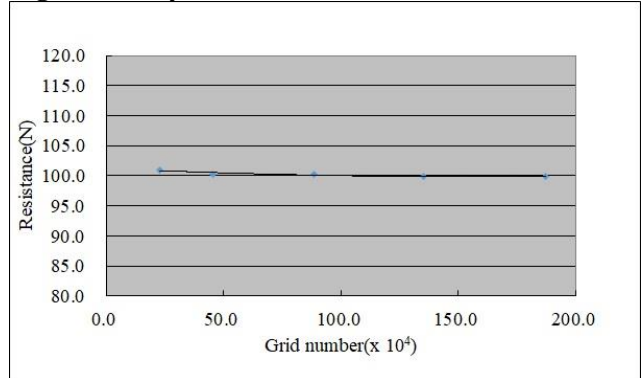

Fig. 5 Check y+ at v=3.045 m/s

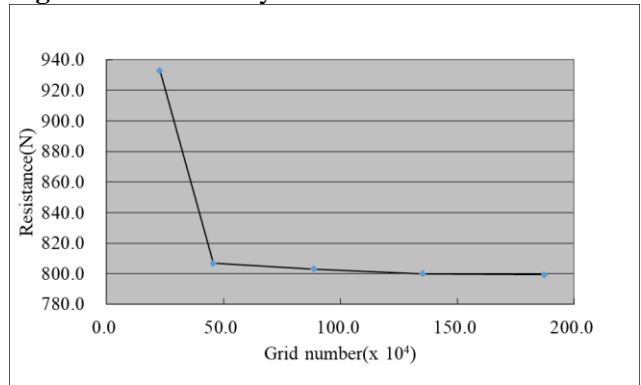**Fig. 6** Grid Sensitivity at v=3.045 m/s

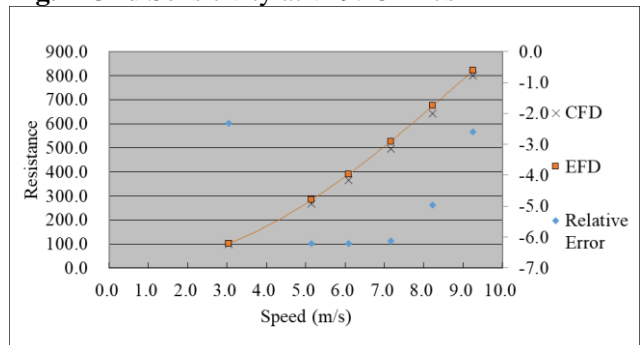**Fig. 7** Grid Sensitivity at v=9.254 m/s

Fig. 8 Comparison with the EFD of DTMB

Generally, the results of CFD showed great agreement with that of experiments in DTMB. The resistance using the CFD solver would be underestimated with the maximum of 6.2% relative error in 5.144 m/s and 6.09 m/s. However, the accuracy has been strong enough to preliminarily acquire the resistance performance of the submarine in the design

stage.

4.2 Open water Test

In this part, the tuned propeller was calculated and comparison with the INSEAN experimental data was shown in Figure 9. The distribution of pressure coefficient was shown in Figure 10.
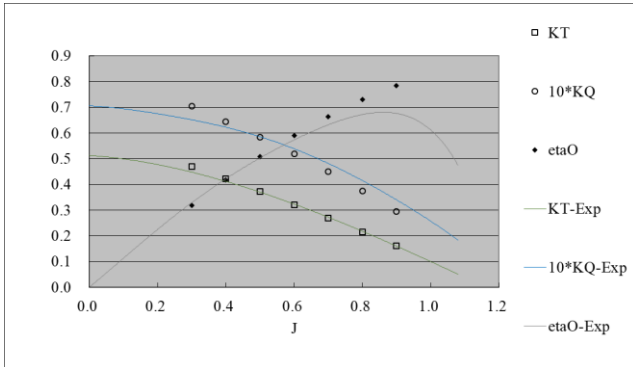
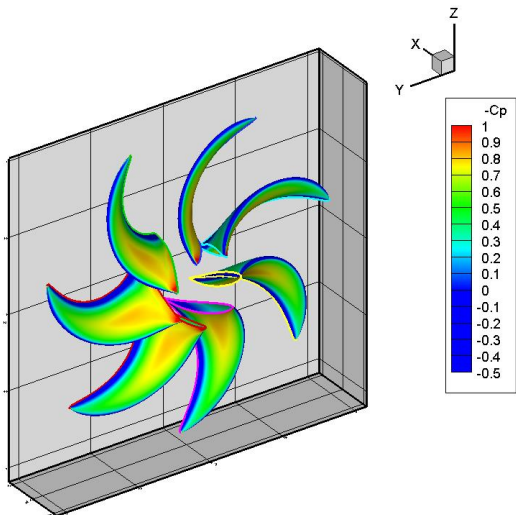**Fig. 9** Comparison with the experiment value of IN-SEAN

Fig. 10 Pressure coefficient of the tuned propeller

4.3 Self-propulsion Test

In this part, the flow of whole computational domain was simulated by using three method.

Because of the consideration of the propeller model, the computational domain should be full flow domain.
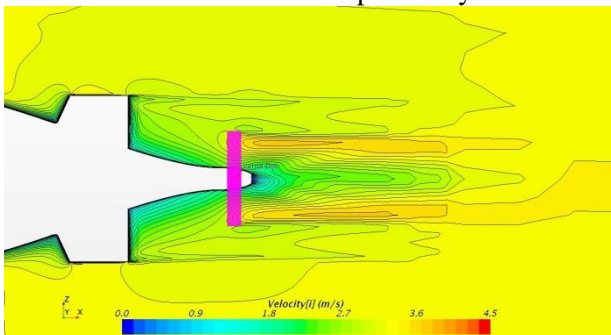
The results were listed independently as follow:

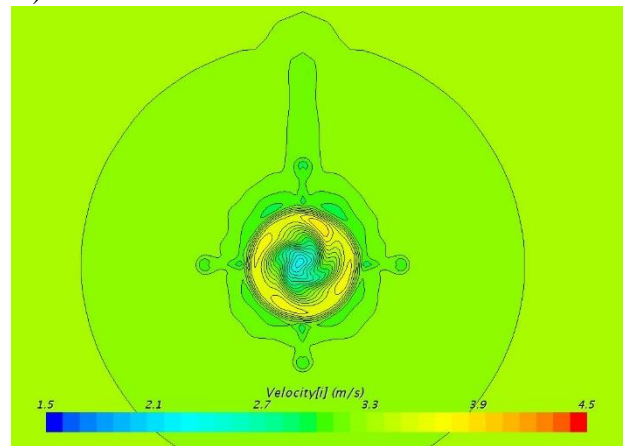**Fig. 11** Cross section plan view of the wake(Method A)

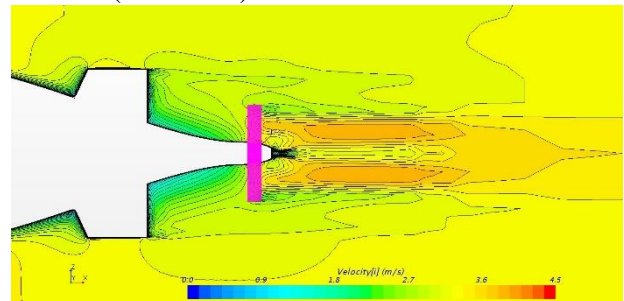**Fig. 12** Wake at $0.05L_{OA}$ behind the center of the virtual disk(Method A)

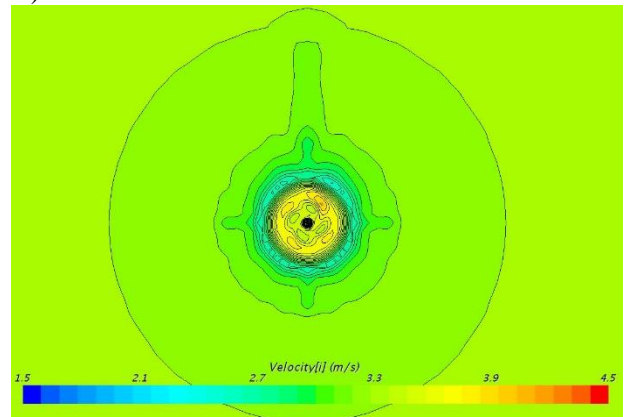**Fig. 13** Cross section plan view of the wake(Method B)

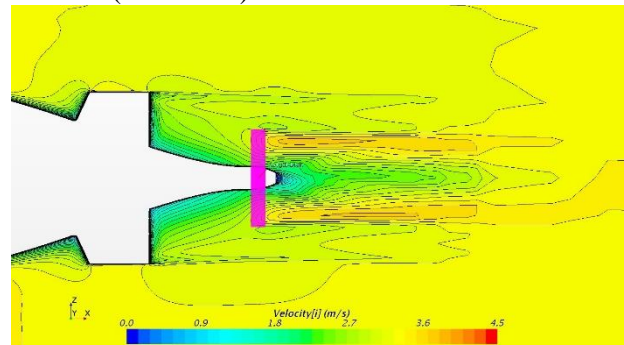**Fig. 14** Wake at $0.05L_{OA}$ behind the center of the virtual disk(Method B)

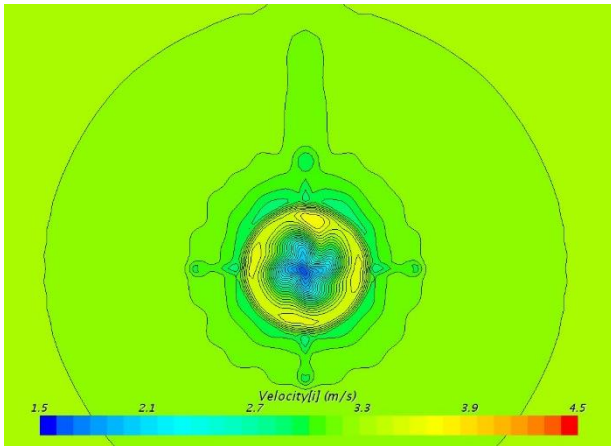**Fig. 15** Cross section plan view of the wake(Method C)

Fig. 16 Wake at $0.05L_{OA}$ behind the center of the virtual disk(Method C)

The wake profile of Method A and C was similar because they used the same calculating method with only the input propeller characteristic slightly different.

In the Method A and C, a number of propeller loading conditions have been calculated with variation of rotational rate, which was shown in the Figure 17.
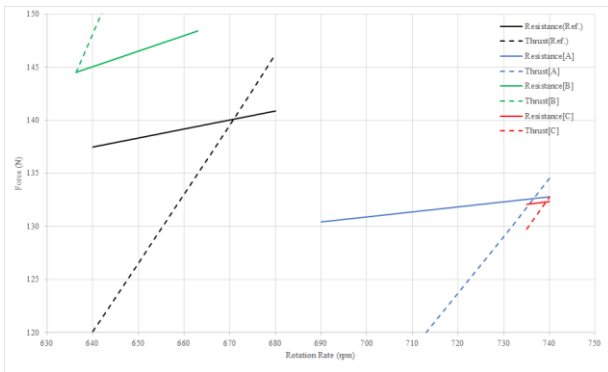

Fig. 17 Self propulsion result at v=3.3436 m/s

Lastly, the results including thrust deduction factors and wake fractions are listed in Table 3.

Table 3 Self propulsion solutions of each method at at v=3.3436 m/s

	t	w	J	n (rps)
A	0.10	0.173	0.859	12.28
B	0.17	0.253	0.899	10.61
C	0.10	0.175	0.855	12.32

5. Conclusion and Future Works

In the present paper, numerical analysis of propulsion for submarine with highly skewed propeller is presented. Propulsion simulation was then conducted and by changing the advance coefficient to obtain the self-propulsion condition. The resistance results at intermediate speed region of CFD showed great agreement with that of experiments in DTMB. Maximum relative error is less than 7%, while the propeller's torque coefficient was overestimated in the lower advance coefficient and underestimated in the lightly loaded condition. Three propulsion configurations had large differences in thrust forces and rotation speed. More detail study of the flow field is necessary for future validations:

- Comparisons with simulation using the real geometry of the INSEAN E1619.
- Verification with the submarine propeller model whose self-propulsion experiment data is available.

References

Chase, N., 2012, Simulations of the DARPA Suboff Submarine Including Self-propulsion with the E1619 propeller'. M.Sc. Thesis, University of Iowa, USA.

D. C. Wilcox, 1993, "Turbulence modeling for CFD", DCW Industries Inc., La Canada, California, USA.

Di Delice, F., Felli, M., Liefvendahl, M. & Svennberg, U., 2009, Numerical and Experiment Analysis of the Wake Behavior of a Generic Submarine Propeller, Proceedings of the 1st International Symposium on Marine Propulsors, Trondheium, Norway.

Groves, N., Huang, T. & Chang, M., 1998, Geometric Characteristics of DARPA SUBOFF Models (DTRC Model Nos. 5470 and 5471. David Taylor Research Center Report, Report No. DTRC/SHD-1298-01, March.

Huang, T. T., Wang, H. T., Santelli, N. and Groves, N. C., 1976., Propeller/Stern Boundary Layer Interaction on Axis-symmetric Bodies: Theory and Experiment, Technical Report DTNSRDC 76-0113, DTNSRDC

ITTC, 2011, "Practical guidelines for ship CFD applications," Proceedings of 26th ITTC, Rio de Janeiro.

Liu, H.-L, Huang, T.T., 1998,. Summary of DARPA SUBOFF Experiment Program Data. Report No. CRDKNSWC/HD-1298-11, June.

Sinan Burunsuz1, M. Cansın Özden1, Yasemin Arıkan Özden2, İsmail Hakkı Helvacıoğlu1, 2017, Four Quadrant Thrust and Torque Prediction of INSEAN E-1619 Generic Submarine Propeller for Submarine Maneuvering Simulations, Fifth International Symposium on Marine Propulsors smp'17, Espoo, Finland.

Y. Cengel and J. M. Cimbalak, 2008, Essentials of fluid mechanics: fundamentals and applications, McGraw-Hill Higher Education.

SIEMENS, 2006, STAR-CCM+ v11.06Theory Guide